*Pathogens and Disease*, 76, 2018, ftx125

doi: 10.1093/femspd/ftx125
Advance Access Publication Date: 26 December 2017
Research Article

RESEARCH ARTICLE

# *Salmonella* escapes antigen presentation through K63 ubiquitination mediated endosomal proteolysis of MHC II via modulation of endosomal acidification in dendritic cells

Mayuri Gogoi[1], Visweswaran Ravikumar[2], Narendra M. Dixit[3,4] and Dipshikha Chakravortty[1,4,*]

[1]Department of Microbiology and Cell Biology, Indian Institute of Science, Bangalore-560012, India, [2]Division of Biological Sciences, Indian Institute of Science, Bangalore-560012, India, [3]Department of Chemical Engineering, Indian Institute of Science, Bangalore-560012, India and [4]Centre for Biosystems Science and Engineering, Indian Institute of Science, Bangalore-560012, India

*Corresponding author: Department of Microbiology and Cell Biology, Indian Institute of Science, Bangalore-560012, Karnataka, India. Tel: +91 80 22932842; E-mail: dipa@iisc.ac.in

**One sentence summary:** Evasion of antigen presentation by *Salmonella* by employing endosomal proteolysis of MHC II.

**Editor:** Willem van Eden

## ABSTRACT

$CD4^+$ T-cell response is vital for successful clearance of *Salmonella* Typhimurium infection. Efficient antigen presentation is crucial for effective $CD4^+$ T-cell response. Previous study has reported that *Salmonella* abrogates antigen presentation capacity of dendritic cells in order to escape host adaptive immune response. In this study, we have elucidated the mechanism of *Salmonella*-mediated downregulation of the total cellular Major Histocompatibility Complex (MHC) II pool in dendritic cells. Infected dendritic cells show upregulation of E3 ubiquitin ligase, MARCH1 expression and K63-linked ubiquitination of MHC II. *Salmonella* infection also enhances the internalisation of ubiquitin-tagged MHC II molecules that are subsequently degraded by endosomal proteases. In addition, *Salmonella* regulates the activation of endosomal proteases by lowering the pH of endosomes. In infected dendritic cells, *Salmonella* delays NOX2 recruitment to the phagosomes thereby preventing its alkalinisation. NOX2 is a significant part of innate immune response against pathogens as it is responsible for Reactive Oxygen Species (ROS) production. In this study, we have demonstrated how *Salmonella* evades MHC II-mediated adaptive immune response in dendritic cells through enhanced endosomal proteolysis. To escape host $CD4^+$T response, *Salmonella* delays NOX2 recruitment, an innate immune response element to the phagosomes.

**Keywords:** dendritic cells; T cells; MHC class II; ubiquitination; antigen presentation/processing

## INTRODUCTION

*Salmonella enterica* is the etiological agent for various diseases spanning from self-limiting diarrhoea to systemic infections like typhoid fever. Global estimates indicate 21 million typhoid cases ever year (Bhutta and Threlfall 2009) and 93 million (Majowicz *et al.* 2010) non-typhoidal *Salmonella* diseases, making it a

**Received:** 11 October 2017; **Accepted:** 22 December 2017

major cause of mortality and morbidity in developing and underdeveloped countries. *Salmonella* infection is primarily contracted through ingestion of contaminated food or water or due to close contact with infected/carrier individuals (Hornick 1970). Once ingested, *Salmonella* can invade the intestinal barrier by infecting M cells and intestinal epithelial cells (Broz, Ohlson and Monack 2012). Alternatively, luminal bacteria are sampled by dendritic cells (DCs) (Rescigno *et al.* 2001). Post colonisation, the bacteria disseminate through the reticuloendothelial system and reside in host macrophages, DCs, polymorphonuclear cells and hepatic cells (Coburn, Grassl and Finlay 2007). DCs form the nodal point during salmonellosis, as they are pivotal for bacterial colonisation, systemic dissemination and host adaptive immune responses. Notably, among the professional Antigen Presenting Cells, only DCs are capable of activating both naive and primed T cells (Ni and O'Neill 1997). This makes DCs relevant in both primary and secondary immune responses against any pathogen. In due course of infection, *Salmonella* manipulates the host by injecting various virulence effectors through the type III secretion system (T3SS) into the host cell. Among all the T3SS, *Salmonella* pathogenicity island I (SPI-I)-encoded T3SS1 is crucial for host cell invasion (Hernandez *et al.* 2004). During its intracellular life, *Salmonella* survives and proliferates in *Salmonella*-containing vacuole (SCV), a modified endosome. *Salmonella* pathogenicity island II (SPI-2)-encoded T3SS2 is crucial for intracellular survival (Waterman and Holden 2003).

For successful clearance of *Salmonella* infection, induction of both $CD4^+$ and $CD8^+$ T-cell responses is necessary (Ravindran and McSorley 2005). In particular, $CD4^+$ T cells appear to play a vital role in mitigating *Salmonella* infection as mice compromised in $CD4^+$ T-cell responses show higher organ burden and succumb to the infection faster (Hess *et al.* 1996). T-cell receptor (TCR) recognition of antigenic peptide–Major Histocompatibility Complex (MHC) II complexes along with co-stimulatory signals results in the activation of $CD4^+$ T cells. MHC II pathway presents exogenous antigens to $CD4^+$ T cells. Biosynthesis of $\alpha$ and $\beta$ chains of MHC II molecules occurs in the endoplasmic reticulum (ER). Within ER, $\alpha$ and $\beta$ chains along with invariant chain (Ii) assemble into a nonomeric $(\alpha\beta\text{Ii})_3$ complex. These nonomeric complexes are trafficked to the trans-Golgi network and further to the endolysosomal compartment (Roche and Furuta 2015). Alternatively, these complexes are directly trafficked to the cell surface. Subsequently, from the plasma membrane they are internalised in an AP-2-dependent manner and targeted to the endolysosomal compartment. The Ii chain is degraded in the endolysosomal compartment to form the CLIP peptide. Further, exogenous antigens derived replace the CLIP peptides and the peptide-loaded MHC II complexes are trafficked to the cell surface for presentation to TCRs (Roche and Furuta 2015). This complex nature of MHC II-mediated antigen processing and presentation provides pathogens a plethora of opportunities to interfere with antigen presentation and escape host adaptive immune responses.

The majority of the insight into *Salmonella* pathogenesis is derived from *Salmonella* Typhimurium infections in mice. This model mimics systemic typhoid disease in humans. *Salmonella* infection of murine bone marrow derived DCs (BMDCs) abrogates the capacity of DCs to present antigen to T cells. A previous report has suggested that this reduction of antigen presentation is due to compromised MHC II-dependent antigen processing (Cheminay, Mohlenbrink and Hensel 2005). In addition, studies on human DCs have shown that *S.* Typhimurium reduces the cell surface MHC II levels (Mitchell *et al.* 2004; Lapaque *et al.* 2009; Van Parys *et al.* 2012). However, the mechanism with which *S.* Typhimurium impairs MHC II-dependent antigen presentation in BMDC is yet unknown. In this study, we elucidate the pathway by which *S.* Typhimurium reduces MHC II expression and antigen presentation in infected DCs.

## MATERIALS AND METHODS

### Cell culture, antibodies and primers

BMDCs were cultured as previously described (Cheminay, Mohlenbrink and Hensel 2005). Briefly, bone marrow from the femurs and tibias were collected aseptically from C57BL/6 mice. Cells were cultured for 6 days in RPMI-1640 containing 10% heat inactivated Fetal Bovine Serum (FBS), 20 ng/ml mouse Granulocyte Monocyte (mGM)-Colony Stimulating Factor (CSF) (Peprotech), 50 $\mu$M $\beta$-mercaptoethanol, 100 U/ml penicillin and 100 $\mu$g/ml streptomycin. Cells were incubated at 5% $CO_2$ and 37°C. After 3 days, mGM-CSF containing media was supplemented. Loosely adherent cells were collected on the sixth day and used for further experiments (Inaba *et al.* 1992). DC purity was 65% to 80%.

Peripheral blood mononuclear cells were isolated from blood buffy coats using Hisep LSM 1077 (HiMedia). After Phosphate Buffered Saline (PBS) washing and RBC lysis, cells were cultured for 6 days similarly as BMDC culture, except that mGM-CSF was replaced by human Granulocyte Monocyte CSF. Loosely adherent cells were collected on the sixth day and used for further experiments.

Anti-mouse CD11c PE-conjugated (BD Pharmingen (#557401)), anti-human CD1c (BD Pharmingen (#564900)) and anti-human HLA-DR,DP,DQ (BD Pharmingen (#555557)) antibodies were used for flow cytometry experiments. Anti-mouse IA/IE (BD Pharmingen (#556999)) antibody was used for immunofluorescence microscopy, flow cytometry, immunoprecipitation and immunoblotting. Anti-K48-linked polyubiquitin (CST (#4289S)), anti-K63-linked polyubiquitin (Enzo life science (#BML-PW0600)) and anti-ubiquitin (Novus Biological (#NB300–130)) antibodies were used for immunoblotting and immunofluorescence microscopy.

For qPCR of MHC II forward primer 5′-ACCAATGAGGC TCCTCAAGC-3′, reverse primer 5′-AAGCAGATGAGGGTGTTGGG-3′, MARCH1 forward primer 5′-GACAATGGTGTGCTGGAATGG-3′, reverse primer 5′-CACAAAGATCACACGGTTGTA-3′, $\beta$-actin forward primer 5′-CAGCAAGCAGGAGTACGATG-3′, reverse primer 5′-GCAGCTCAGTAACAGTCCG-3′ and GAPDH forward primer 5′-GACAACTTTGGCATTGTGGAA-3′, reverse primer 5′-GGATGCAGGGATGATGTTCTG-3′ were used.

### Bacterial strains and infection

*Salmonella* Typhimurium 14028 (ATCC) was grown overnight at 37°C, 160 rpm. DCs were infected with stationary-phase bacterial culture with an MOI 10. To synchronise the infection, tissue culture plates were subjected to centrifugation at 500 × *g* for 5 min. Cells were washed with PBS and were treated with RMPI-1640 + 10% FBS containing 50 $\mu$g/ml gentamicin for 1 h. Subsequently, the gentamicin concentration was reduced to 10 $\mu$g/ml and maintained until the cells were harvested. Bafilomycin (50 nM), folimycin (1 $\mu$M), chloroquine (15 $\mu$M), MG132 (0.5 $\mu$M) and leupeptin hemisulfate (10 $\mu$M) were added along with RMPI-1640 containing 10% FBS, 10 $\mu$g/ml gentamicin and maintained until the cells were harvested.

## Flow cytometry and immunofluorescence

Cells were fixed with 3.5% paraformaldehyde (PFA) for 15 min. All staining was performed in the presence of a permeabilising agent, 0.5% saponin (Sigma) dissolved in 2.5% BSA containing PBS unless mentioned otherwise. Flow cytometry analysis was done using BD Canto II, and data analysis was carried out in Denovo platform. Mean fluorescence intensity was calculated in the CD11c-positive population. All immunofluorescence images were obtained using Zeiss LSM 750 and were analysed using the ZEN black 2012 platform. Mander's colocalisation co-efficient was calculated for region of interest.

## Quantitative real-time PCR

Analysis of gene expression was cried out using qPCR. Briefly, RNA from DCs was isolated using TRIzol (Takara) as per the manufacture's protocol. mRNA was reverse transcribed to cDNA using oligo (dT)18 primer and Tetro reverse transcriptase (Bioline) as per protocol. The expression profile of desired gene was evaluated using specific primers (as mentioned in Appendix) by qPCR SYBR master Mix (Takara) in Applied Biosystems ViiTM7 Real time PCR instrument.

## ELISA

Estimation of IL-10 in conditioned media was performed according to the manufacturer's instructions. Briefly, 96-well ELISA plates (BD Bioscience) were coated overnight with capture antibody (BD Bioscience (#555252)) at 4°C. Next day, plates were washed with 0.1% tween-20 containing PBS and blocked with 10% FBS for 1 h. Following blocking wells were washed and incubated with 100 $\mu$L of test samples (conditioned media) for 2 h at room temperature. Subsequently, plates were washed and incubated with detection antibody and enzyme reagent for 1 h at room temperature. TMB (sigma) was used as a substrate, and reactions were stopped with 2 N $H_2SO_4$. Absorbance was measured at 450 nm wavelength, and a concentration of IL-10 was interpolated from a standard curve.

## Immunoprecipitation and immunoblot

For immunoprecipitation, DCs were infected with an MOI 10 as mentioned previously. After 10 h post infection, cells were washed with PBS and were lysed in native lysis buffer containing 1% Nonidet P-40, 20 mM Tris (pH 8), 2 mM EDTA, 150 mM NaCl and protease inhibitors mixture (Roche Diagnostics) for 30 min at 4°C. Cell debris was removed by centrifugation at 10 000 rpm for 10 min, and supernatant was treated with anti I-A/I-E (clone M5/114.15.2) antibody (BD Bioscience). Antibody–MHC II complexes were immunoprecipitated using Protein G linked Sepharose beads (Sigma). Beads were extensively washed with washing buffer and denatured at 95°C for 10 min. Denatured precipitates were subjected to SDS-PAGE (12% gel) followed by transfer to 0.45 $\mu$ PVDF membrane. The membrane was blocked using 5% skimmed milk in TTBS for 1 h at room temperature. ECL (Bio Vision) was used for detection, and images were captured using ChemiDoc GE healthcare.

All the densitometry analyses were performed using Image J platform. For polyubiquitin blots, ubiquitin bands were normalised with the corresponding MHC II band.

## MHC II internalisation assay

For internalisation assay, DCs were infected with *Salmonella* for 25 min. Surface MHC II was labelled with I-A/I-E (clone M5/114.15.2) antibody (BD Bioscience) for 1 h at 4°C. After labelling, cells were washed with cold PBS to remove any unbound antibody and were treated with RPMI-1640 containing 10% FBS and 10 $\mu$g/ml gentamicin and were chased at 37°C. Cells were harvested and fixed with 3.5% PFA at different time points. After fixation, surface antibody–MHC II complexes were blocked with anti-rat secondary antibody in the absence of saponin. Subsequently, cells were washed with PBS and internalised antibody–MHC II complexes were stained with alexa647 dye conjugated anti-rat secondary antibody in the presence of 0.05% saponin. After staining, cells were washed with PBS and flow cytometry was performed.

For immunofluorescence imaging, after the chase period, cells were stained with alexa647 dye conjugated anti-rat secondary antibody in the presence of 0.05% saponin along with anti-*Salmonella* and anti-K63 linkage-specific antibody.

## *In vivo* infection

Six-week-old male C57BL/6 mice were either infected with $10^7$ bacteria or mock infected via oral gavage. The animal experiments were carried out in accordance with the approved guidelines of the institutional animal ethics committee at Indian Institute of Science, Bangalore, India (Registration No: 48/1999/CPCSEA). All the experiments involving the use of animals were performed according to Institutional Animal Ethics Committee approved protocol. Five days post infection, spleens were collected. For splenic DCs, spleens were mechanically disintegrated and RBC lysis was performed. The adherent cell population was fixed with PFA. DCs were gated in a flow cytometer by using DC marker CD11c. MHC II levels were quantified in the splenic DC subpopulation.

## Cryosectioning and fluorescence immunohistochemistry

For immunohistochemistry, 5 days post infection, spleens were collected and fixed with 4% PFA. Fixed tissues were embedded in optimal cutting temperature compound and cryosectioning was performed in –20°C. Cryosections were sequentially stained with anti-*Salmonella*, anti-MHC II, anti-CD11c antibody and respective secondary antibodies at 4°C. After staining, images were acquired in a Zeiss LSM 710 microscope.

## Comparison of endosomal/lysosomal pH

In order to compare the endosomal/lysosomal pH, infected and control cells were stained with 100 nM Lysotracker green -DND-26 (Life technologies) for 45 min at 37°C. Cells were washed harvested followed by flow cytometry analysis at 504/511 nm.

## Comparison of *Salmonella* containing vacuole pH and endosome

pH of SCV was analysed according to the previous report (Chakraborty *et al.* 2014). Bacterial or ovalbumin were labelled with 20 $\mu$M pH rodo red succinimidyl ester (Invitrogen) at 37°C for 1 h. Bacteria were washed with 0.1 M sodium bicarbonate buffer (pH 8.4) before and after labelling. DCs were infected with

labelled bacteria (MOI 10) for 25 min, and non-internalised bacteria were washed away with PBS followed by gentamicin treatment. Cells were washed, and flow cytometry analysis was carried out at 560/585 nm in BD Canto II.

### Reactive Oxygen Species (ROS) measurement

Intracellular ROS quantification was performed by 2′,7′-Dichlorofluorescin diacetate ($H_2$DCFDA) (Sigma) staining. Cells were stained with 10 $\mu$M $H_2$DCFDA at 37°C in dark. After 20 min, cells were washed with ice-cold PBS and harvested followed by flow cytometry analysis at 495/530 nm in Canto II.

### Statistical analysis

Statistical analyses were performed with the GraphPad Prism software. Student's *t*-test was performed as indicated. The results are expressed as mean ± SD or mean ± SEM. Group sizes, experiment number and *P* values for each experiment are described in the figure legends.

## RESULTS

### *Salmonella* Typhimurium infection mediates downregulation of total MHC II pool in DCs

*Salmonella* Typhimurium infection of BMDCs suppresses antigen presentation. Infected DCs show compromised antigen presentation of ovalbumin to Ova specific T cell (Tobar, Gonzalez and Kalergis 2004; Cheminay, Mohlenbrink and Hensel 2005) suggesting the involvement of MHC II. To determine the effect of *Salmonella* infection on MHC II expression, we compared both surface and total MHC II levels between infected and uninfected DCs using flow cytometry and immunofluorescence microscopy. Total MHC II and surface MHC II pool were stained with anti-MHC II antibody either in the presence or absence of 0.01% saponin, a pore-forming agent, respectively. *Salmonella* infection results in the reduction in both surface (Fig. S1B, Supporting Information) and total MHC II pools (Fig. 1A–C) as compared to uninfected and PFA-fixed bacteria-treated samples at 20 h post infection. The decrease in the total MHC II level can be attributed to either downregulation of MHC II synthesis or upregulation of MHC II degradation. qPCR analysis of MHC II expression did not show significant change in infected DCs compared to uninfected DCs (Fig. S1C, Supporting Information). This indicates the role of MHC II degradation rather than MHC II synthesis. MHC II, in general, shows ubiquitin-mediated degradation and, hence, we next examined the ubiquitination status of MHC II. Immunoblot of MHC II immunoprecipitate showed two distinct bands of molecular weight ∼60 kDa and ∼35 kDa. Different ubiquitin chain lengths attached to MHC II molecules can be a probable explanation for the presence of multiple bands (Fig. S2A, Supporting Information). Hence, the next question was to understand the ubiquitination status of MHC II in infected DCs.

### *Salmonella* Typhimurium infection enhances MARCH1-mediated ubiquitination of MHC II

MHC II is a heterodimer of $\alpha$ (33–35 kDa) and $\beta$ (25–30 kDa) chains, and ubiquitination of lysine 225 present on the cytoplasmic domain of the MHC II $\beta$-chain is critical for MHC II degradation. The length of lysine 225 conjugated ubiquitin is a major determinant in MHC II internalisation and degradation (Ma *et al.* 2012). The presence of two different molecular weight bands in the MHC II immunoprecipitate (Fig. 2A) can be attributed to different ubiquitin chain lengths. In order to examine the ubiquitination status, MHC II immunoprecipitates from infected and control DCs were probed with anti-ubiquitin antibody. Both the populations of MHC II showed conjugated ubiquitin. In contrast with previous reports, MHC II populations corresponding to only two molecular weights were detected in our study. Furthermore, anti-ubiquitin antibody probing detected only two bands and no ubiquitin ladder was detected in the MHC II immunoprecipitate (Fig. 2A). The absence of unqbiquitinated MHC II might be due to insufficient resolution of mono and unubiquitinated MHC II. To address this issue, we have subjected MHC II immunoprecipitate to a 15% SDS-PAGE gel and carried out immunoblot analysis with both MHC II and ubiquitin antibody. Long exposure of the immunoblot shows poly, mono, and un-ubiquitinated MHC II fraction (Fig. S1D, Supporting Information); however, the un-ubiquitinated band lowest molecular weight is not stained by anti-ubiquitinated antibody (Fig. S1E, Supporting Information). As the molecular weight of the MHC II $\beta$ chain is 25–30 kDa, the ∼35 kDa and ∼60 kDa bands might represent monoubiquitinated and quadramer of ubiquitin in $\beta$ chains, respectively. A recent study has established the role of MHC II ubiquitin length in MHC II endocytosis and lysosomal targeting in DCs (Ma *et al.* 2012). In contrast to oligoubiquitinated MHC II, monoubiquitinated MHC II are less efficiently internalised. Therefore, further immunoblot analysis was carried out for the polyubiquitinated MHC II pool (∼60 kDa). We found that *Salmonella* infection of DCs resulted in ∼2-fold increase in MHC II polyubiquitination compared to control (Fig. 2B). Immunofluorescence analysis also shows higher colocalisation of ubiquitin with MHC II in infected cells compared to uninfected or PFA-fixed *Salmonella*-treated samples (Fig. 2C and D). The role of polyubiquitination in MHC II internalisation has been previously implicated (Shin *et al.* 2006). Following our observation that *Salmonella* enhances polyubiquitination of MHC II, we next investigated the effect of *Salmonella* infection on MHC II internalisation. To study the endocytosis of MHC II, surface MHC II was labelled with anti-MHC II antibody for 1 h at 4°C. After antibody labelling, unbound antibody was removed by PBS wash and cells were chased at 37°C for the desired time and cells were subsequently fixed with PFA. These DCs contain three subsets of MHC II: (i) surface MHC II–antibody complex, (ii) internalised MHC II–antibody complex and (iii) intracellular free MHC II. Surface MHC II-antibody complexes were blocked using alexa488 conjugated secondary antibody. For staining of internalised MHC II–antibody complexes, cells were treated with the pore-forming agent, saponin. Pores formed on the cell membrane allowed alexa647 conjugated secondary antibody to stain internalised MHC II–antibody complexes. Hence, the alexa647 intensity is a direct indication of internalised MHC II–antibody complexes and alexa488 intensity indicates surface MHC II. In our study, infected cells show ∼2.4-fold and ∼4-fold higher internalisation of MHC II compared to uninfected and PFA killed bacteria-treated sample, respectively (Fig. 2E and F). Concomitantly, we also observe a decrease in un-internalised surface MHC II in STM-infected cells as compared to control (Fig. 2G and H). Thus, the *Salmonella*-mediated increase in polyubiquitination of MHC II correlates with its enhanced internalisation MHC II in DCs.

Enhanced ubiquitination requires increased levels of E3 ubiquitin ligase activity. In BMDCs, MHC II ubiquitination is largely performed by membrane associated RING-CH (MARCH) 1, an E3 ubiquitin ligase (Cho *et al.* 2015). It is a short-lived protein with a half-life of <30 min. During activation of DCs, transcription of MARCH1 is suppressed, resulting in decreased

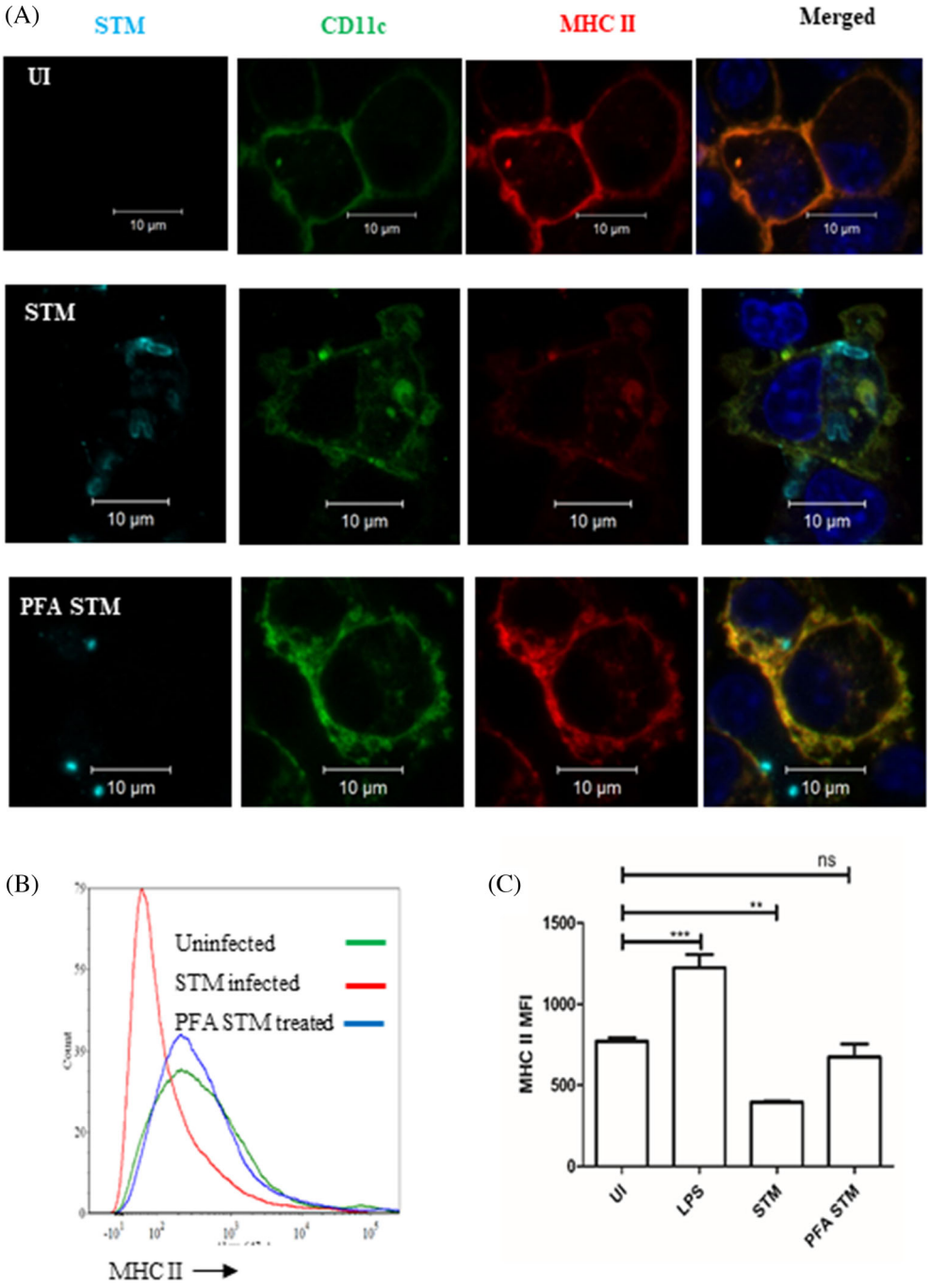


**Figure 1.** *Salmonella* Typhimurium infection mediates downregulation of MHC II in DCs. (**A**) Representative confocal images of DCs showing total MHC II levels at 20 h post infection. DCs were stained for total MHC II in the presence of 0.01% saponin (see also Fig. S1B and C, Supporting Information). (**B**) Representative flow cytometry histogram showing total MHC II levels at 20 h post infection. DCs were stained for total MHC II in the presence of 0.01% saponin. (**C**) MFI of total MHC II levels at 20 h post infection. DCs were stained for total MHC II in the presence of 0.01% saponin. Data are presented as mean ± SD of one experiment, representative of three independent experiments (see also Fig. S1B) (unpaired two tailed Student's *t* test, *P* value, *** <0.0001, ** <0.001). UI, uninfected; LPS, lipopolysaccharide; STM, infected, PFA STM, paraformaldehyde-fixed *Salmonella* Typhimurium.

ubiquitination of MHC II (Jabbour *et al.* 2009). In this study, q-PCR analysis of MARCH1 gene showed a biphasic transcriptional regulation. Compared to control cells, infected DCs showed up-regulation of MARCH1 expression till 6 h post infection. However, at 20 h post infection, the levels were not different from uninfected control. Notably, treatment with lipopolysaccharide, an activation signal, resulted in downregulation of MARCH1 expression (Fig. 2I). Thus, it follows that *Salmonella* infection enhances polyubiquitination of the total MHCII pool by upregulating MARCH 1 expression. Previous study has emphasised on the role of IL-10 in DC maturation and MHC II expression (de Waal Malefyt *et al.* 1991). The ability of IL-10 to upregulate MARCH1 expression is previously reported in murine DCs (Tze *et al.* 2011) and human monocytes (Thibodeau *et al.* 2008). Pathogens such

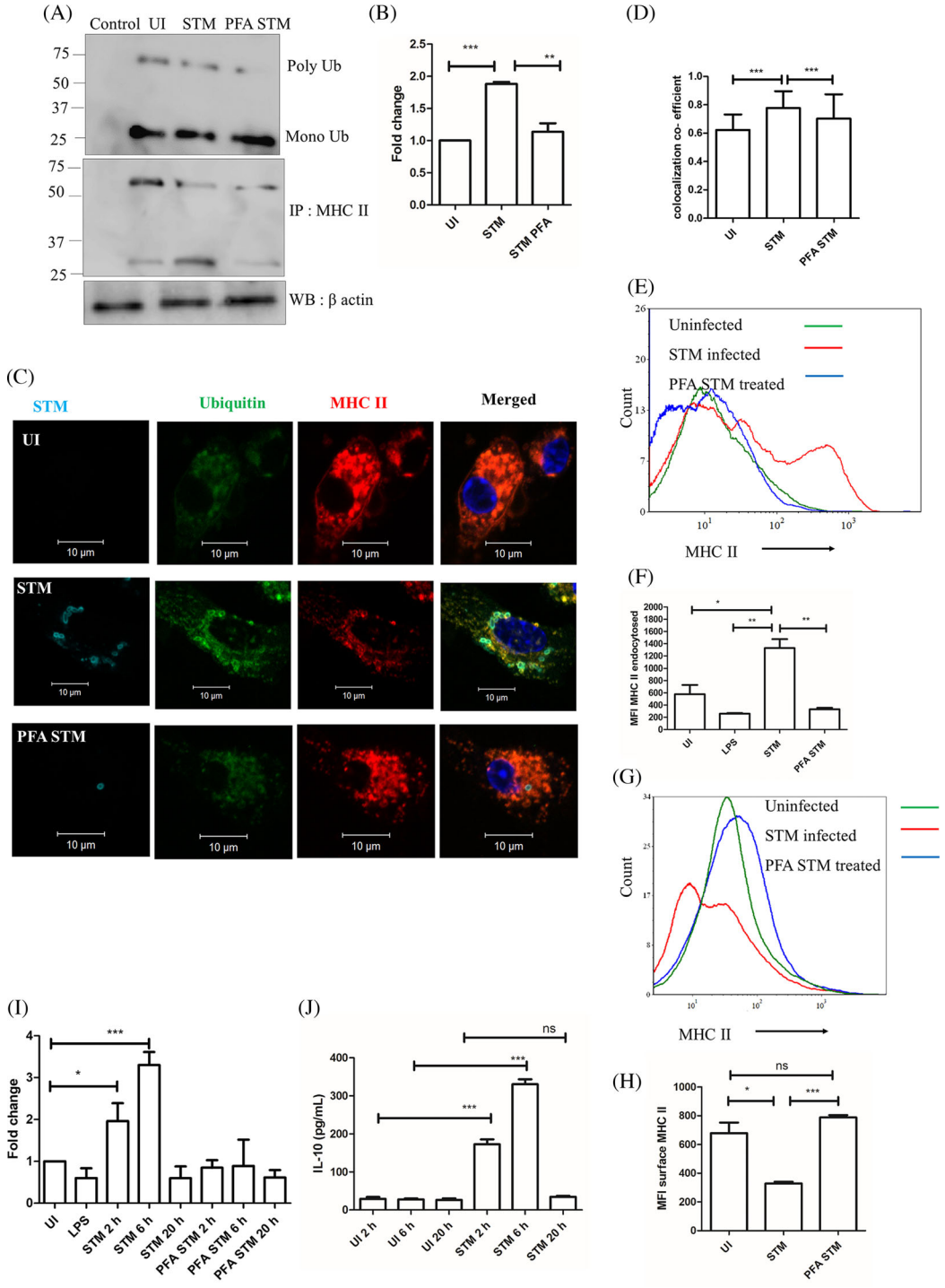


**Figure 2.** *Salmonella* Typhimurium infection enhances the ubiquitination of MHC II. (**A**) Immunoblot analysis of polyubiquitination of MHC II immunoprecipitate at 10 h post infection. MHC II was immunoprecipitated from infected and control DCs and probed for MHC II and ubiquitin. (**B**) Densitometry analysis of polyubiquitination of MHC II immunoprecipitate at 10 h post infection. MHC II was immunoprecipitated from infected and control DCs and probed for MHC II and ubiquitin. Data are presented as mean ± SD of three independent experiments. (**C**) Confocal image showing ubiquitination status of MHC II at 20 h post infection by immunofluroscence. DCs were stained for total MHC II and ubiquitin in the presence of 0.01% saponin. (**D**) Quantification of MHC II and ubiquitination colocalisation at 20 h post infection. DCs were stained for total MHC II and ubiquitin in the presence of 0.01% saponin (n = 184). (**E**) Representative flow cytometry histogram showing internalisation of surface labelled MHC II. Surface MHC II were labelled for 1 h at 4°C and chased for 1 h at 37°C. (**F**) MFI showing internalisation of surface labelled MHC II. Surface MHC II were labelled for 1 h at 4°C and chased for 1 h at 37°C. Data are presented as mean ± SD of one experiment, representative of five independent experiments. (**G**) Representative flow cytometry histogram showing un-internalised surface labelled MHC II. Surface MHC II were labelled for 1 h at 4°C and chased for 1 h at 37°C. (**H**) MFI showing un-internalised surface labelled MHC II. Surface MHC II were labelled for 1 h at 4°C and chased for 1 h at 37°C. Data are presented as mean ± SD of one experiment, representative of three independent experiments. (**I**) qPCR analysis of MARCH1 gene expression at indicated time post infection. (Data are presented as mean ± SEM of three independent experiments). (**J**) IL-10 ELISA of conditioned media at indicated time point post infection. (Data are presented as mean ± SEM of four independent experiments) (unpaired two tailed Student's *t* test, *P* value, *** <0.0001, ** <0.001, * <0.01). UI, uninfected; LPS, lipopolysaccharide; STM, infected, PFA STM, paraformaldehyde-fixed *Salmonella* Typhimurium.

as murine cytomegalovirus affect MHC II expression in infected cells via enhancing IL-10 expression in infected cells (Redpath *et al.* 1999). Thus, we have investigated whether MARCH1 regulation correlates with secreted IL-10 profile in infected cells. Indeed, ELISA of conditioned media confirms our hypothesis that IL-10 levels in cell supernatant are upregulated at 2 h and 6 h as compared to uninfected control (Fig. 2J). This result might indicate towards the role of IL-10 in MARCH1-dependent downregulation of MHC II.

## *Salmonella* infection enhances lysine 63-linked ubiquitination of MHC II

The interubiquitin linkage in polymeric ubiquitin chains plays a pivotal role in determining the fate of ubiquitinated proteins. Lysine 48-linked ubiquitin-tagged proteins are generally subjected to proteasomal degradation and lysine 63-linked ubiquitin-tagged proteins are targeted for cellular trafficking (Zinngrebe *et al.* 2014). To address the fate of ubiquitinated MHC II in infected DCs, MHC II immunoprecipitate was probed with both K63 and K48 ubiquitin linkage-specific antibodies. Infected DCs showed ∼2-fold increase in K63-linked polyubiquitination compared to control. However, unlike K63-linked ubiquitination, there was no change in K48-linked ubiquitination (Fig. 3A–C; Fig. S2A and B, Supporting Information). Immunofluorescence analysis also showed colocalisation of MHC II and K63-linked ubiquitination (Fig. 3D). These results emphasise the role of intracellular trafficking in *Salmonella*-mediated MHC II downregulation. MHC II trafficking is a dynamic process where intracellular MHC II is trafficked to the cell surface and surface MHC II is constantly internalised and either degraded or recycled back to the surface (van Niel *et al.* 2006). Therefore, we next addressed the role of K63-linked ubiquitination in internalisation of MHC II. The surface MHC II was labelled with anti-MHC II antibody at 4°C followed by chase at 37°C. Staining of MHC II–antibody complex and K63 ubiquitin in the presence of saponin provided us insight into the ubiquitination status of the surface and internalised MHC II. Indeed, infected DCs showed more internalisation of MHC II–antibody complexes compared to control and internalised MHC II more strongly colocalised with K63 linkage-specific ubiquitin antibody in infected cells compared to control (Fig. 3E and F). K63-linked ubiquitination of MHC II, therefore, plays a key role in MHC II internalisation and degradation.

## Endosomal proteolysis is responsible for *Salmonella*-mediated total MHC II downregulation

In order to delineate the ubiquitinated MHC II degradation pathway, cells were subjected to either proteasomal inhibitor MG132 or endosomal acidification inhibitor (bafilomycin, folimycin and chloroquine). MG132 treatment did not rescue *Salmonella*-mediated downregulation, thus ruling out the involvement of proteasomal degradation. In contrast, treatment with endosomal acidification inhibitor rescued MHC II levels significantly, indicating the role of endosomal degradation (Fig. 4A and B). For endosomal degradation of MHC II, the most likely candidate is endosomal proteolysis. To test whether endosomal protease is essential for *Salmonella*-mediated abrogation of MHC II, we have treated the infected cells with leupeptin hemisulfate, a serine/cysteine protease inhibitor. Indeed, leupeptin treatment rescued MHC II levels in infected cells (Fig. 4C and D). These data confirm the role of endosomal proteases in MHC II downregulation during *Salmonella* infection.

*In silico* analysis using PROSPER further confirms the presence of cathepsin K (cysteine protease) and cathepsin G (serine protease) cleavage site on MHC II. Previously, the ability of cathepsin G to degrade MHC II *in vitro* has been reported (Fig. 4E) (Burster *et al.* 2010).

## Role of endosomal acidification on MHC II downregulation

To prevent their deleterious effect, endosomal proteases are synthesised as zymogens. An inhibitory motif blocks the zymogen's active site. Low pH causes release of the active site, which is either followed by inhibitory motif's autodigestion or cleavage by other active endoproteases. Although activation of endosomal proteases requires low pH, most of these proteases are functional over a broad pH range (Chapman 2006; Turk *et al.* 2012). The fact that endosomal acidification inhibitors could rescue MHC II levels highlights the role of pH in endosomal proteolysis of MHC II. To confirm this, we examined the acidification status of endosomes using lysotracker DND-26 dye. Intriguingly, at an early time point (30 min), the pH of endosomes was more acidic in infected DCs compared to control (Fig. 5A and B). However, this difference in pH was not observed at a later time point (Fig. 5C). This result also supports our hypothesis that lower pH is a requirement for activation of zymogens rather than for their function. Similarly, at an early time point (30 min), pH rodo conjugated bacteria also showed low pH in SCV, a modified phagosome, compared to pH in phagosome containing PFA-fixed bacteria (Fig. 5D and E; Fig S4A, Supporting Information). In addition, we have labelled ovalbumin with pH rodo to analyse the endosomal pH. Ovalbumin–pH rodo complex once internalised will enter endosomal trafficking pathway, and the pH rodo fluorescence indicates the acidification status of the endosomes. Our results suggest that STM-infected cells have more acidic pH than that of uninfected and PFA STM-treated cells (Fig. 5F and G). All these lines of evidence confirm the role of phagosomal and endosomal pH in endosomal proteolysis and subversion of antigen presentation.

## Delay in NOX2 recruitment is crucial for MHC II downregulation

DC phagosomes recruit NADPH oxidase 2 (NOX2) to their membranes, which in turn makes the phagosomes less acidic compared to macrophage phagosomes. Once recruited, NOX2 generates superoxide ions, which are converted to hydrogen peroxide by the enzyme, superoxide dismutase. During this process, $H^+$ ions present in the phagosomal lumen are consumed, driving an increase in pH (Savina *et al.* 2006). Immunofluorescence microscopy of DCs showed delayed recruitment of NOX2 to SCV compared to phagosomes containing PFA-fixed bacteria (Fig. 6A–C). Estimation of intracellular ROS also showed decreased levels in *Salmonella*-infected cells compared to fixed bacteria-treated cells at 30 min post infection (Fig. 6D and E). If a delay in NOX2 recruitment is essential for lowering of pH and hence for protease activation, then NOX2 null DCs treated with PFA-fixed bacteria should also show a reduction in total MHC II levels. Indeed, BMDCs derived from gp91phox$^{-/-}$ (NOX2 KO) mice showed decreased total MHC II levels even in PFA-fixed bacteria-treated samples, thus confirming the role of NOX2 in *Salmonella*-mediated MHC II downregulation. This is further supported by the fact that

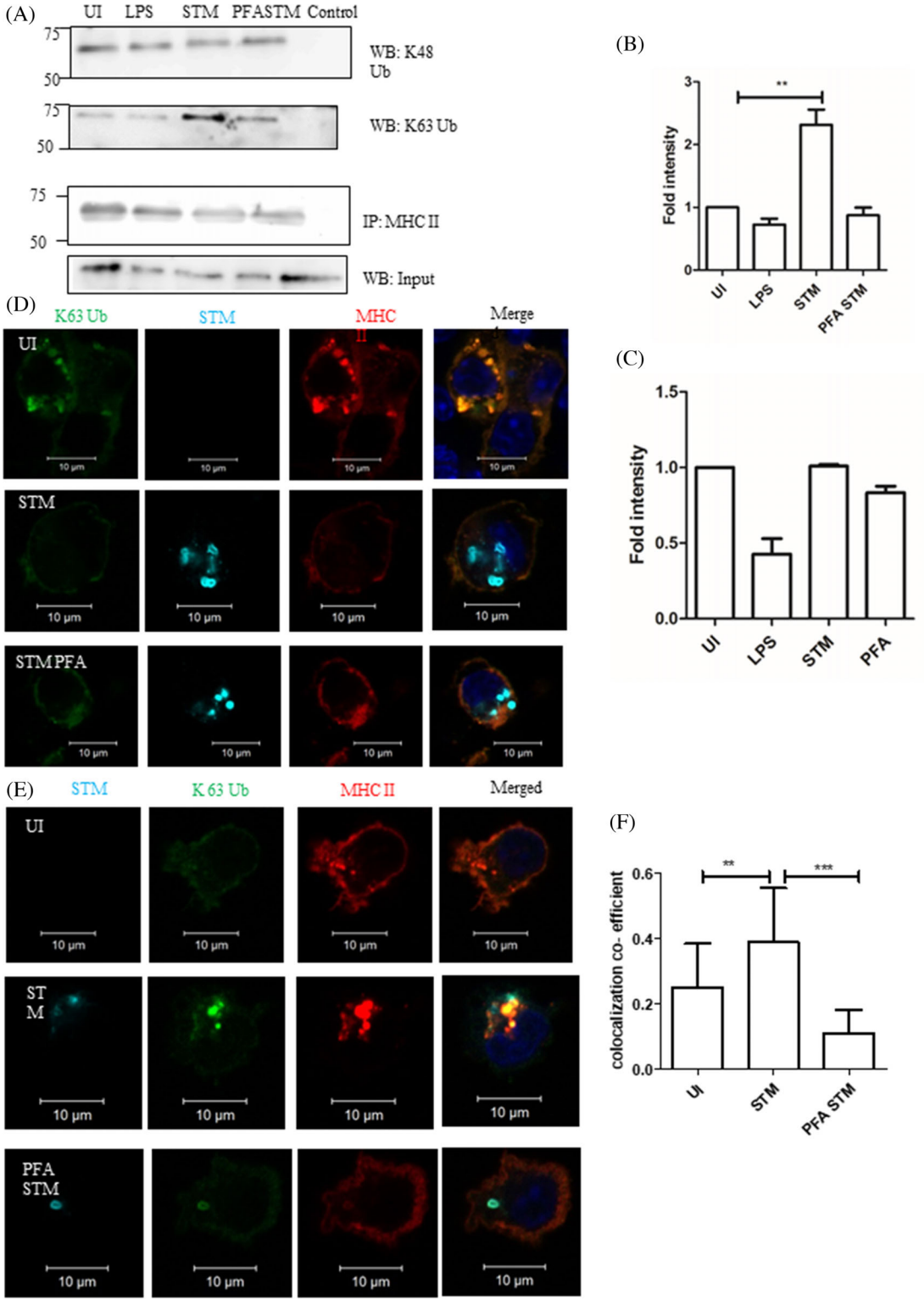


**Figure 3.** *Salmonella* infection enhances lysine 63-linked ubiquitination of MHC II. (**A**) Comparison of K63 and K48-linked polyubiquitination status of MHC II immunoprecipitate at 10 h post infection. MHC II immunoprecipitates were probed for MHC II, K63 and K48-linked polyubiquitination by immunoblot (see also Fig. S2A and B, Supporting Information). (**B**) Densitometry analysis of K63-linked polyubiquitination status of MHC II immunoprecipitate at 10 h post infection. MHC II immunoprecipitates were probed for MHC II, K63 and K48-linked polyubiquitination by immunoblot. Data are presented as mean ± SD of three independent experiments. (**C**) Densitometry analysis of K48-linked polyubiquitination status of MHC II immunoprecipitate at 10 h post infection. MHC II immunoprecipitates were probed for MHC II, K63 and K48-linked polyubiquitination by immunoblot. Data are presented as mean ± SD of three independent experiments. (**D**) Confocal image showing K63-linked ubiquitination and MHC II in DCs. (**E**) Confocal image showing K63-linked ubiquitination status of internalised MHC II. (**F**) Colocalisation of K63-linked ubiquitin and internalised MHC II (n = 50) (unpaired two tailed Student's *t* test, *P* value, *** <0.0001, ** <0.001, * <0.01). UI, uninfected; STM, *Salmonella* Typhimurium infected; PFA STM, paraformaldehyde fixed *Salmonella;* Control, Ig control.

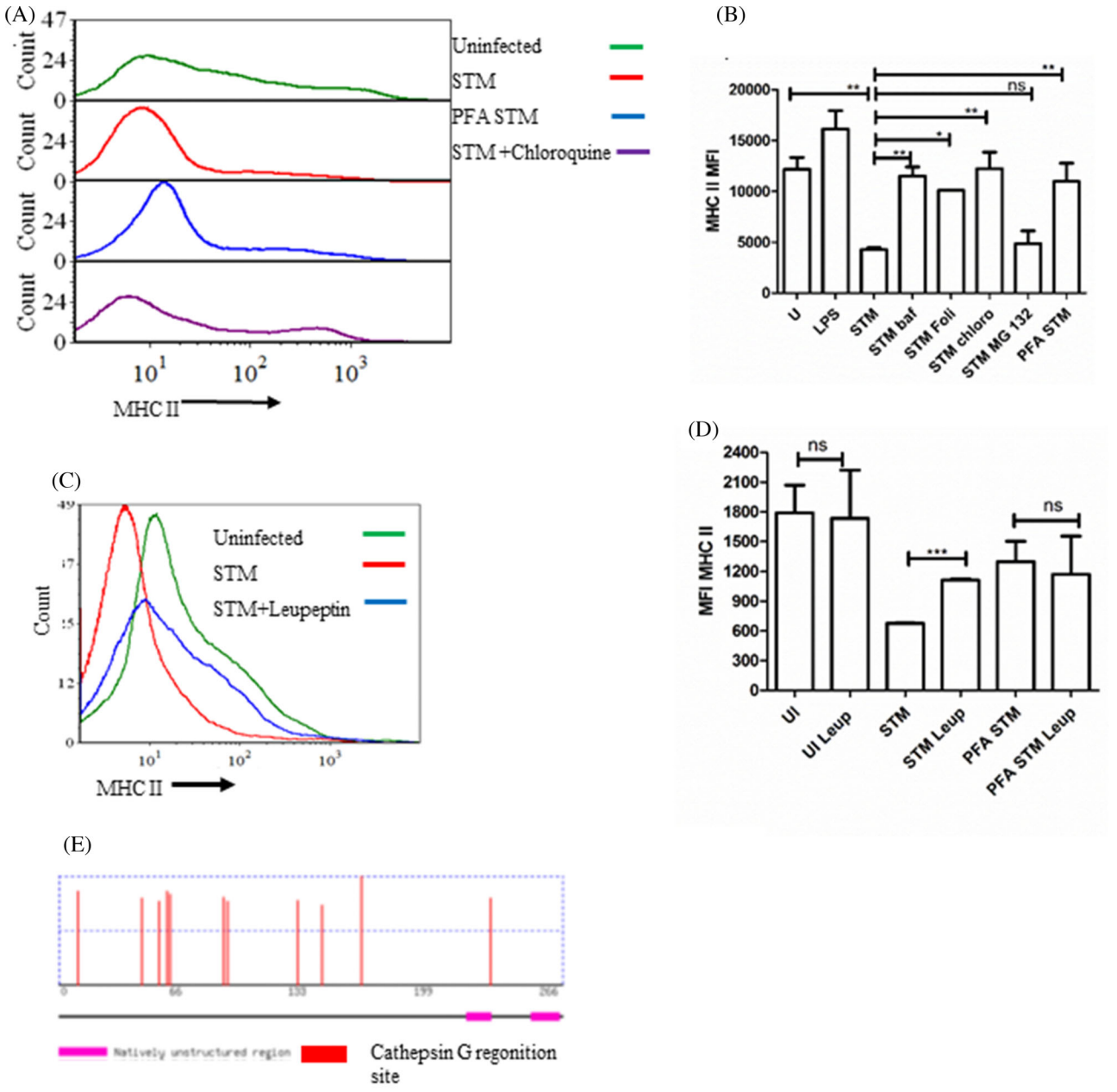


**Figure 4.** Endosomal proteolysis is responsible for *Salmonella*-mediated total MHC II downregulation. (**A**) Representative flow cytometry histogram showing total MHC II level in response to endosomal acidification inhibitor and proteosomal inhibitor treatment in infected DCs at 20 h post infection. (**B**) MFI of total MHC II level in response to endosomal acidification inhibitor and proteosomal inhibitor treatment in infected DCs at 20 h post infection. Data are presented as mean ± SD of one experiment, representative of five independent experiments (see also Fig. S3A and B, Supporting Information). (**C**) Representative flow cytometry histogram showing the effect of leupeptin hemisulfate treatment on *Salmonella*-mediated reduction of total MHC II level in DCs at 20 h post infection. (**D**) MFI total MHC II level in DCs at 20 h post infection in response to leupeptin hemisulfate treatment during *Salmonella* infection. Data are presented as mean ± SD of one experiment, representative of four independent experiments (see also Fig. S3B, Supporting Information). (**E**) Cathepsin G recognition site on MHC II (unpaired two tailed Student's *t* test, *P* value, *** <0.0001, ** <0.001, * <0.01). UI, uninfected; STM, *Salmonella* Typhimurium infected; PFA STM, paraformaldehyde fixed *Salmonella;* Baf, Bafilomycin; Foli, Folimycin; Chloro, Chloroquine; MG132, proteosomal inhibitor.

chloroquine treatment can rescue MHC II expression, even in gp91phox knockout mice (Fig. 6F and G). In accordance with this, endosomes of Gp91phox$^{-/-}$ DCs treated with fixed bacteria showed more acidic pH compared to wild-type DC (Fig. 6H and I).

In order to confirm the role of temporal ROS regulation in MHC II degradation, we treated the cells with 0.1 $\mu$M $H_2O_2$ for 1 h post infection. Indeed, this resulted in the rescue of total MHC II levels in infected cells (Fig. S4B, Supporting Information). Collectively, these results suggest that *Salmonella*-mediated temporal regulation of intra-endosomal ROS is a crucial strategy for evasion of antigen presentation.

## *Salmonella* Typhimurium-infected DCs show downregulation of MHC II *in vivo*

To determine whether similar to *ex vivo* experiments *S.* Typhimurium infection can contribute to downregulation of MHC

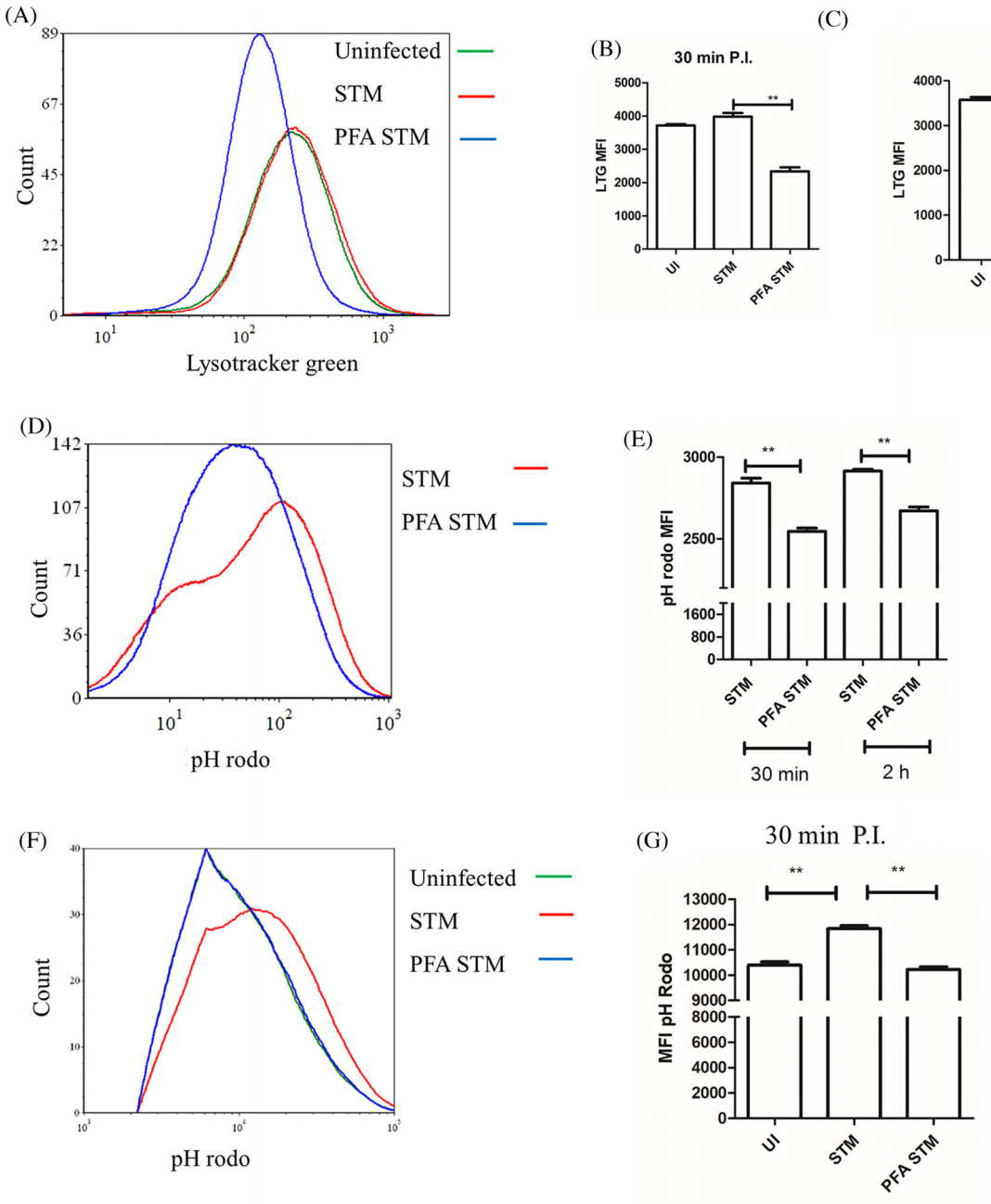


**Figure 5.** Role of endosomal acidification on MHC II downregulation. (**A**) Representative flow cytometry histogram showing comparison of endosomal pH with acid tropic dye lysotracker green at 30 min post infection by flow cytometry. (**B**) MFI of lysotracker green quantification at 30 min post infection. Data are presented as mean ± SEM of four independent experiments (see also Fig. S4E and F, Supporting Information). (**C**) MFI of lysotracker green quantification at 20 h post infection. Data are presented as mean ± SEM of three independent experiments. (**D**) Representative flow cytometry histogram showing pH of *Salmonella* containing vacuole at 30 min post infection with flow cytometry. pH rodo conjugated bacteria were used for DC infection, and pH rodo intensity is direct indication of acidification of SCV (see also Fig. S4 C and D, Supporting Information). (**E**) MFI of pH rodo intensity at indicated time point. Data are presented as mean ± SD of one experiment, representative of six independent experiments (see also Fig. S3A, Supporting Information). (**F**) Representative flow cytometry histogram showing pH of endosomes at 30 min post infection with flow cytometry. Internalised pH rodo conjugated ovalbumin intensity is direct indication of acidification of endosomes. (**G**) MFI of pH rodo intensity at indicated time point. Data are presented as mean ± SD of one experiment, representative of three independent experiments (unpaired two tailed Student's *t* test, *P* value, *** <0.0001, ** <0.001, * <0.01). UI, uninfected; STM, *Salmonella* Typhimurium infected; PFA STM, paraformaldehyde fixed *Salmonella*.

II *in vivo*, C57BL/6 mice were challenged with $10^7$ CFU bacteria or PBS. CD11c-positive DCs from infected mice spleen showed a significant reduction in total MHC II as compared to splenic DCs from control mice (Fig. 7A and B). However, this decrease in MHC II expression was a global effect as uninfected DCs isolated from *Salmonella*-infected mice also express reduced levels of total MHC II. Immunohistochemistry of spleen cryosections with anti-CD11c and anti-MHC II and anti-*Salmonella* antibody also substantiate the decrease in total MHC II expression in DCs in the infected spleen compared to control (Fig. 7C).

Both *S.* Typhimurium and *S.* Typhi are human pathogens. However, only *S.* Typhi can cause systemic infection in humans;

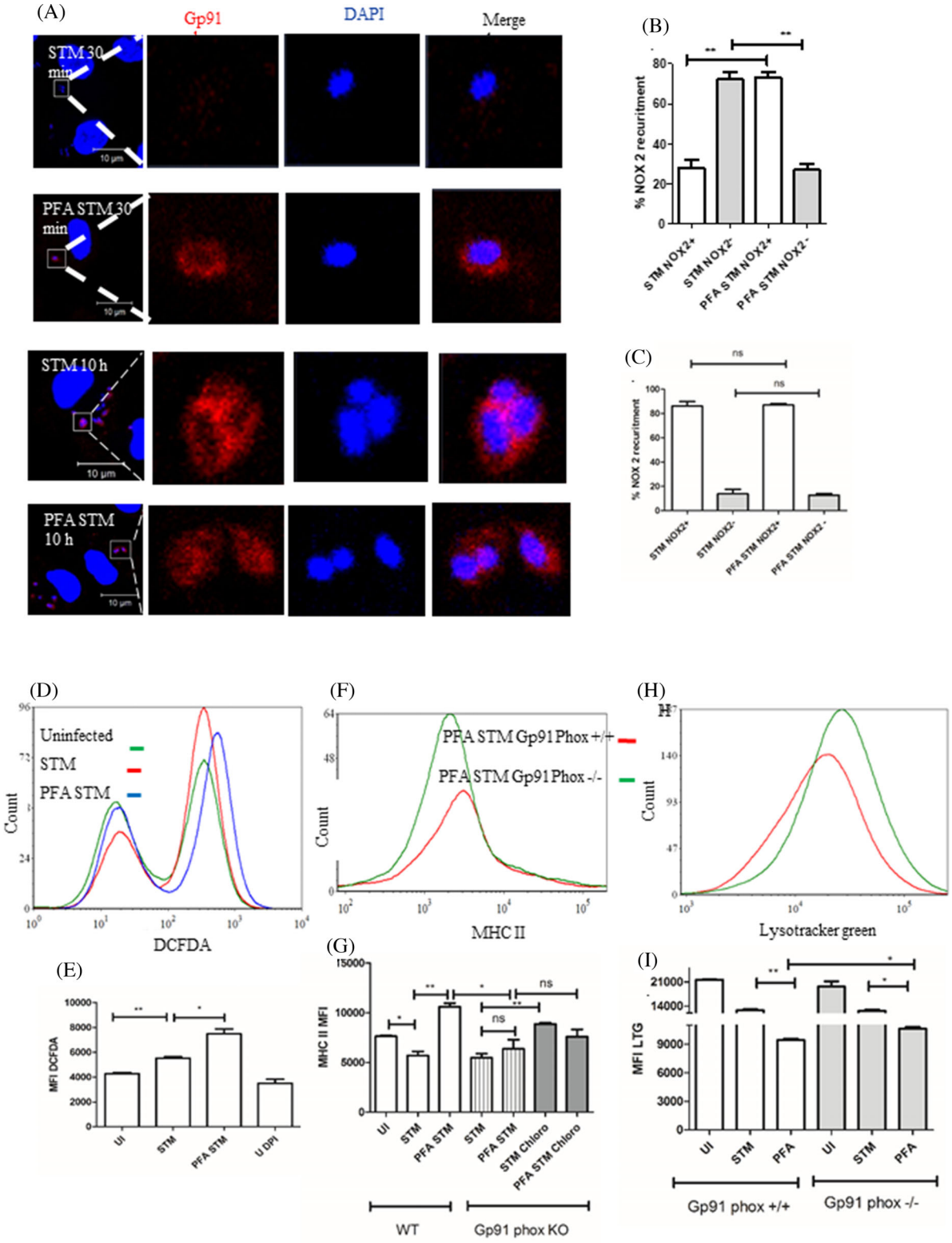


**Figure 6.** Delay in NOX2 recruitment is crucial for MHC II downregulation. (**A**) Confocal image of NOX2 recruitment to phagosomal membrane at 30 min and 10 h post infection by immunofluorescence. (**B**) Quantification of NOX2 recruitment to phagosomal membrane (N = 3) at 30 min post infection. (**C**) Quantification of NOX2 recruitment to phagosomal membrane (N = 3) at 10 h post infection. (**D**) Representative flow cytometry histogram showing intracellular ROS level with H2DCFDA at 30 min post infection. (**E**) MFI of H2DCFDA at 30 min post infection. Data are presented as mean ± SEM of four independent experiments. (**F**) Representative flow cytometry histogram showing endosomal pH in WT and Gp91 Phox KO DCs. Endosomal pH was assessed by lysotracker green at 30 min post infection. (**G**) MFI of lysotracker green at 30 min post infection in WT and Gp91 Phox KO DCs. Data are presented as mean ± SEM of three independent experiments. (**H**) Representative flow cytometry histogram showing *Salmonella*-mediated MHC II downregulation in WT and Gp91 Phox KO DCs at 20 h post infection. (**I**) MFI of total MHC II in WT and Gp91phox KO DCs at 20 h post infection. Data are presented as mean ± SD of one experiment, representative of two independent experiments. UI, uninfected; STM, *Salmonella* Typhimurium infected; PFA STM, paraformaldehyde fixed *Salmonella;* Chloro, chloroquine.

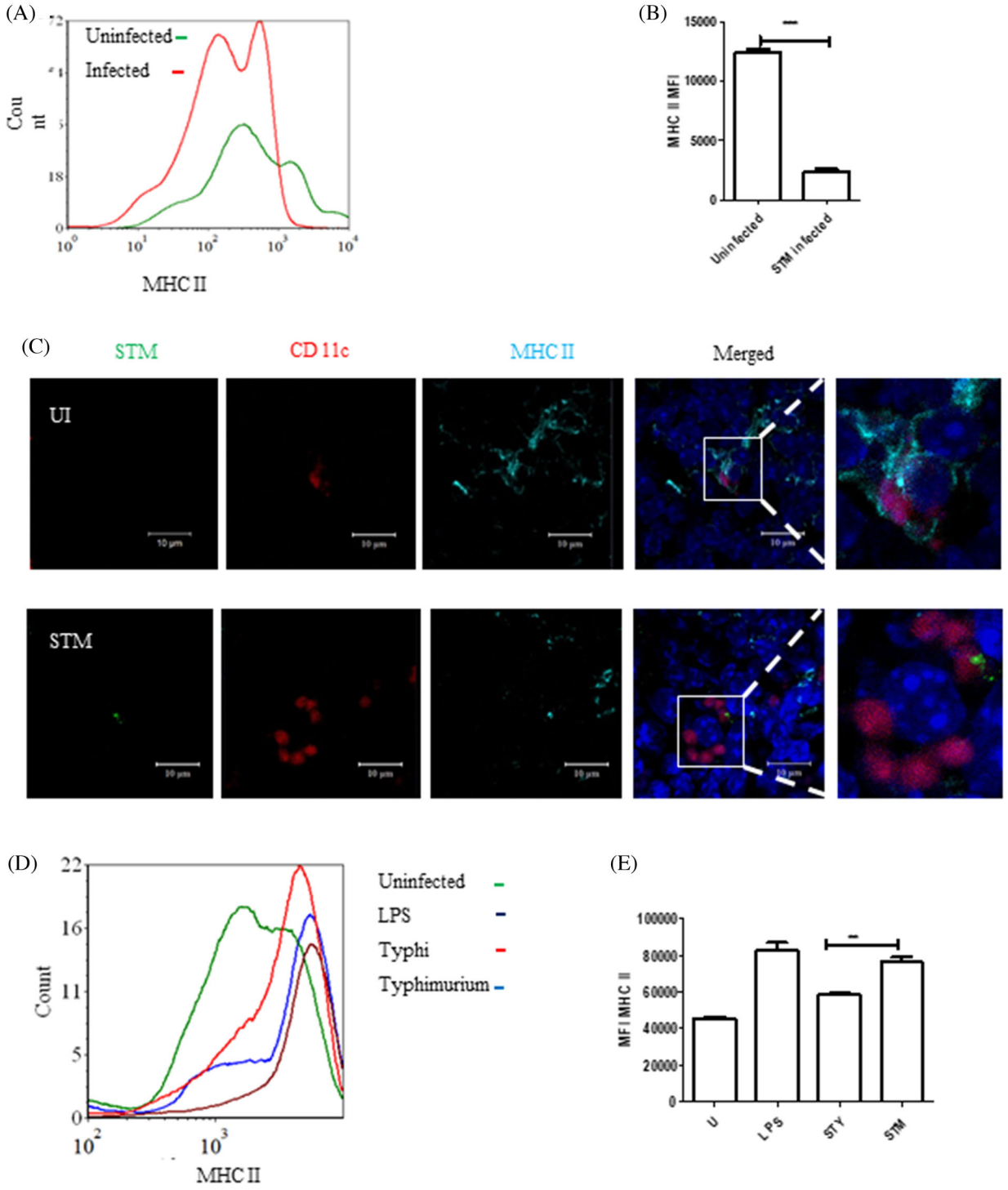


**Figure 7.** *Salmonella* infection downregulates MHC II in DCs *in vivo*. (**A**) Representative flow cytometry histogram of total MHC II in splenic DCs isolated from infected and uninfected mice. (**B**) MFI of total MHC II in splenic DCs isolated from infected mice. Data are presented as mean ± SD of one experiment, representative of three independent experiments. (**C**) Immunohistochemistry of spleen. (**D**) Representative flow cytometry histogram of total MHC II of S. Typhimurium and S. Typhi mediated MHC II downregulation in DC at 20 h post infection, representative flow cytometry experiment. (**E**) MFI of total MHC II of S. Typhimurium and S. Typhi-mediated MHC II downregulation in DC at 20 h post infection, representative flow cytometry experiment. Data are presented as mean ± SD of one experiment, representative of three independent experiments (unpaired two tailed Student's *t* test, *P* value, *** <0.0001, ** <0.001, * <0.01). UI, uninfected; LPS, lipopolysaccharide; STY, *Salmonella* Typhi; STM, *Salmonella* Typhimurium infected.

S. Typhimurium causes self-limiting diarrhoea. *Salmonella* Typhi infection downregulates MHC II expression in human DCs more efficiently than S. Typhimurium (Fig. 7D and E). This suggests that host specificity might be due to the differential ability to regulate antigen presentation by S. Typhi and S. Typhimurium in human and mice DCs.

### Computational modelling of the MHC II trafficking pathway

To identify the strategy used by *Salmonella* to downregulate total MHC II, we developed a mathematical model of MHC II synthesis, trafficking and degradation in DCs (Fig. 8A). A detailed description of the model is provided in supplementary information (Mathematical model supplementary method, model construction). Every parameter in the model was estimated using datasets from the literature, thus making the model consistent with available data on the MHC II trafficking pathway in DCs. Using the model, we simulated the effect of *Salmonella* infection by perturbing the rates of the individual steps in the pathway one at a time to different extents (1.1-fold, 2-fold and 10-fold) in such a way that antigen presentation by peptide-loaded MHC II molecules is compromised. We studied the effect of these perturbations on the total MHC II pool by comparing MHC II levels in infected and uninfected DCs. Model predictions suggested that only downregulation of MHC-II synthesis, upregulation of MARCH1 expression and/or ubiquitination rate have a significant impact on the total MHC II levels both at steady state (Fig. 8B) and transiently following the perturbation (Fig. 8C–E). We confirmed that these predictions are not sensitive to variations in parameter values (Mathematical model supplementary method, sensitivity analysis). Our experimental data indicate that *Salmonella* infection does not affect MHC II synthesis. *Salmonella* infection also enhances MARCH1 expression and ubiquitination of MHC II in DCs. Thus, our mathematical model predictions are in accordance with experimental findings that S. Typhimurium causes downregulation of the total MHC II pool in DCs via ubiquitination of MHC II.

## DISCUSSION

Our study establishes a novel link between endosomal proteolysis of MHC II and delayed NOX2 recruitment to phagosomes in infected BMDCs. *Salmonella* Typhimurium suppresses MHC II presentation by BMDCs as an evasion strategy to subvert host adaptive immune responses. Reduction in surface and total MHC II is the reason for impaired antigen presentation in infected DCs. We and previous study has demonstrate that enhanced MHC II degradation is the primary reason for the reduction of MHC II levels. In murine DCs, MARCH1 is the major E3 ubiquitin ligase involved in MHC II ubiquitination (Walseng *et al.* 2010). In this study, we have observed that *Salmonella* infection induces MARCH1 expression in infected DCs. This result is corroborated by the fact that infected DCs show higher MHC II ubiquitination as compared to control. Previously, McCormick, Martina and Bonifacino (2005) demonstrated that the major pool of newly synthesised MHC II is trafficked via the cell surface to the endosomal system. MHC II $\beta$ chain lysine 225 polyubiquitination provides the signal for its internalisation and degradation (Shin *et al.* 2006; van Niel *et al.* 2006; Balce *et al.* 2011). Indeed, *Salmonella* infection enhances MHC II internalisation. For the first time, in this study, we have demonstrated that *Salmonella* infection enhances K63-linked polyubiquitination of MHC II. On the contrary, there was no change in K48-linked polyubiquitination of MHC II. K63-linked ubiquitination is often associated with cellular trafficking, and K48-linked ubiquitination generally targets proteins for 26 S proteasomal degradation (Zinngrebe *et al.* 2014). Confirming the conventional role of K63 ubiquitination, K63-linked ubiquitinated MHC II shows enhanced internalisation in infected cells. Furthermore, this is the first report to demonstrate the role of endosomal proteolysis in MHC II degradation during *Salmonella* infection of BMDCs. We have also established the role subtle regulation of endosomal pH in determining the fate of MHC II. *Salmonella* infection-mediated downregulation of MHC II also explains one of the mechanisms by which *Salmonella* evades the host immune response. Reduction in MHC II levels directly correlates with reduced antigen presentation and impaired $CD4^+$ T-cell response which is necessary to keep the infection at bay. Rescue of antigen presentation potential by the protease inhibitor, leupeptin hemisulfate, further supports the role of endosomal proteolysis in MHC II processing.

Recent study by Bayer-Santos *et al.* (2016) suggests the role of MARCH8 in ubiquitination of MHC II in Mel JuSo cell line. Although MARCH1 and MARCH8 show 79.4% similarity (Fujita *et al.* 2013), immune cells mainly express MARCH1. Previous studies have also demonstrated that MARCH1 is the designated ubiquitin E3 ligase involved in ubiquitination of MHC II in DCs (De Gassart *et al.* 2008; Walseng *et al.* 2010; Oh *et al.* 2013; ten Broeke, Wubbolts and Stoorvogel 2013) as MARCH8-deficient mice show no change in MHC II levels in DCs and B cells (Oh and Shin 2015). The difference between our findings from Bayer-Santos *et al* might be due to the fact that Mel Juso cell line does not express MARCH1.

Our results also indicate towards involvement of IL-10 in regulation of MARCH1 during *Salmonella* infection. However further investigation is required to elucidate the mechanism involved. The most likely explanation for this is the involvement of effector proteins secreted by *Salmonella* T3SS. This is also supported by the fact that the suppression of antigen presentation by *Salmonella* is an SPI2-dependent process. SPI-2 mutants like Δ*steD* (Bayer-Santos *et al.* 2016) and Δ*ssaV* are impaired in suppressing antigen presentation (Cheminay, Mohlenbrink and Hensel 2005; Halici *et al.* 2008; Lapaque *et al.* 2009; Bayer-Santos *et al.* 2016). It would be interesting to investigate the ability of *Salmonella* to alter the cellular localisation of MARCH1 and the probable role of *steD* in IL-10-mediated MARCH1 regulation. Apart from the upregulation of MARCH1, *Salmonella* infection might regulate host deubiquitinase function, thus resulting in increased ubiquitination of MHC II. The process of internalisation of ubiquitinated MHC II from the surface requires further attention. Previous reports suggest that clathrin and AP-2 are involved in the internalisation of ubiquitinated MHC II (McCormick, Martina and Bonifacino 2005; Walseng, Bakke and Roche 2008). However, the probability of differential trafficking of MHC II polyubiquitin containing endosome in infected cells cannot be ignored. Identification of endosomal proteases involved in MHC II degradation also needs further attention. In the future, this might help in therapeutics, as specific inhibitors of these proteases could be used to boost the immune system along with an antibiotic regime. In addition, previous studies have alluded to the preferential ubiquitination of peptide–MHC II complexes by MARCH1 (Furuta, Walseng and Roche 2013). As our study does not differentiate the degradation of peptide MHC II complex vs MHC II-invariant chain complex, it will be interesting to investigate whether *Salmonella* infection reduces their levels differently. Apart from its active role in infected cells, *Salmonella* infection might orchestrate reduction of MHC II in uninfected cells via

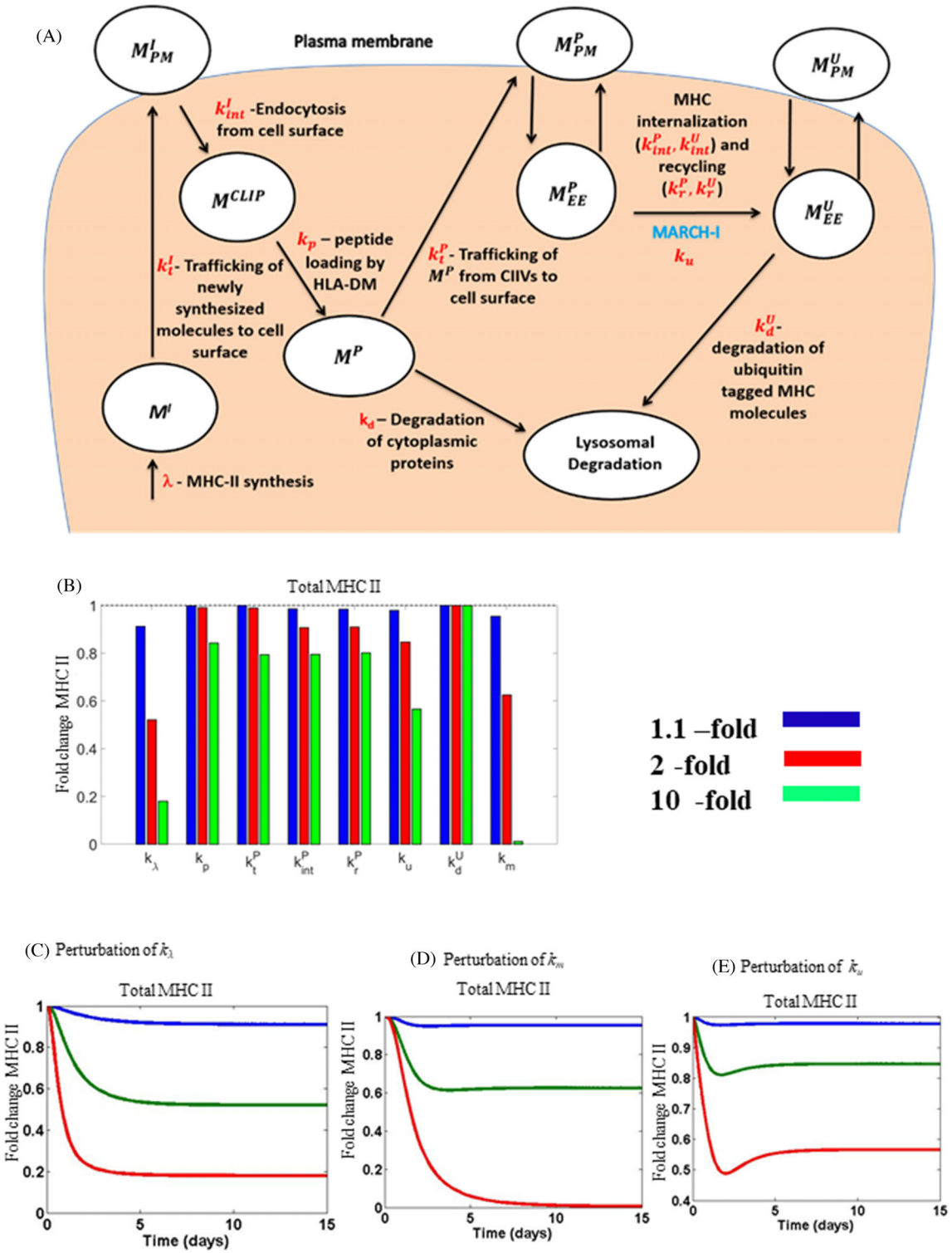


**Figure 8.** Computation modelling of MHC II trafficking pathway. (**A**) Representation of MHC II trafficking in dendritic cells that was used to construct the mathematical model. M: MHC-II molecule, superscript represents state of the molecule and subscript represents location in cell; $M^I$: invariant chain bound; $M^I_{PM}$: invariant chain bound in plasma membrane; $M^{CLIP}$: CLIP peptide bound; $M^P$: antigenic peptide bound; $M^P_{PM}$: peptide bound, in plasma membrane; $M^P_{EE}$: peptide bound, in early endosomes; $M^U_{PM}$: ubiquitinated, in plasma membrane; $M^U_{EE}$: ubiquitinated, in early endosomes. (**B**) The effect of perturbing individual steps of the MHC II trafficking pathway on the steady state total number of MHC molecules in infected cells as a fraction of the number in uninfected DCs. $k_\lambda$—silencing of MHC II synthesis, $k_m$—upregulation of MARCH-I expression, $k_u$—ubiquitination of internalised MHC II, $k^U_d$—degradation of ubiquitin-tagged MHC II, $k_p$—CLIP displacement and antigenic-peptide loading, $k^P_t$ trafficking of peptide-loaded MHC II to cell surface, $k^P_{int}$—internalisation of surface-expressed MHC, $k^P_r$—recycling of internalised MHC II. The steps influenced by these parameters are also shown in A. (**C**) The effect of downregulation of MHC II synthesis rate ($k_\lambda$) on total MHC II kinetics. (**D**) The effect of MARCH1 silencing rate ($k_m$) on total MHC II kinetics. (**E**) The effect of rate of ubiquitination of internalised MHC II ($k_u$) on total MHC II kinetics.

soluble factors like IL-10 secreted by infected cells (Thibodeau *et al.* 2008).

The current study has revealed phagosomal acidification as a mode of regulation for protease activity in DCs. During its maturation, V-ATPases are recruited to the phagosomal membrane. This causes an influx of proton and results in acidification of phagosomal lumen. On the contrary, recruitment of NOX2 to the phagosomal membrane results in sustained ROS production, which causes proton consumption and alkalinisation of the phagosomal lumen. It is the delicate balance between the activity of V-ATPase and NOX2, which determines the pH of the DC phagosome. It has been previously reported that NOX2 recruitment is crucial for regulating the protease activity and thus for the preservation of antigenic epitopes in DCs (Savina *et al.* 2006). The ability of endosomal acidification inhibitors to rescue MHC II levels supports the role of pH in MHC II degradation. Our study revealed the novel mechanism by which NOX2 regulates MHC II degradation. In infected cells, NOX2 recruitment to the endosomes is delayed, thus allowing the luminal pH to acidify. Endosomal pH is crucial in determining endosomal protease activation. This supports our observation that delay in NOX2 recruitment to the endosomes correlates with lower endosomal pH which results in activation of endosomal proteases. However, this difference in pH between infected cells and PFA-fixed bacteria-treated samples is not observed at later time points, which might indicate that lowering of pH is required for activation but not for its action. Alternatively, NOX2 recruitment can influence the activation of endosomal protease by changing the reductive potential of the endosomal lumen. This can regulate the activity of cysteine protease (Balce *et al.* 2011; Rybicka *et al.* 2012). This possibility is highly unlikely as acidification inhibitors can rescue MHC II levels. However, the mechanism by which *Salmonella* delays NOX2 recruitment demands further investigations. In macrophages, *Salmonella* avoids NOX2 recruitment in an SPI-2-dependent manner (Vazquez-Torres *et al.* 2000), a phenomenon supported by the inability of Δ*sseD*, an SPI 2 mutant, in avoiding NOX2 recruitment (Gallois *et al.* 2001).

Altogether, this study provides mechanistic insights on how *Salmonella* manipulates an innate immune component, NOX2, to escape the host's adaptive immune response. This might be of immense importance in explaining recurrent *Salmonella* infections in chronic granulomatosis disease (defect in NOX2) patients. Recurrent bacterial infection in this genetic disease is attributed to defective neutrophil function. However, it is time for researchers to visit this condition from another perspective i.e. the antigen presentation ability of DCs and also to evaluate the role of adaptive immune response in these patients.

## SUPPLEMENTARY DATA

Supplementary data are available at *FEMSPD* online.

## ACKNOWLEDGEMENTS

We are very grateful to Prof. Apurva Sarin, NCBS and Dr Mohan, NCBS for providing Gp91 phox$^{-/-}$ mice. We also appreciate the contribution of Central Animal Facility, Flow cytometry Facility and MCB Imaging Facility.

## Author Contribution

MG has designed experiments, performed experiments and written the manuscript and prepared the figures (Figs 1–7). VR has performed the experiment (Fig. 8) and prepared the figure (Fig. 8). NMD has designed the experiment (Fig. 8) and prepared the figure (Fig. 8). DC has designed experiments and written the manuscript.

## FUNDING

This work was supported by DAE SRC outstanding fellowship to DC and DBT-IISc partnership program for advanced research in biological sciences and bioengineering to DC Infrastructure support from ICMR (Center for Advanced Study in Molecular Medicine), DST (FIST), and UGC (special assistance) is acknowledged. Welcome Trust/DBT India Alliance Senior Fellowship IA/S/14/1/501307 (NMD).

***Conflict of interest.*** None declared.

## REFERENCES

Balce DR, Li B, Allan ER *et al.* Alternative activation of macrophages by IL-4 enhances the proteolytic capacity of their phagosomes through synergistic mechanisms. *Blood* 2011;**118**:4199–208.

Bayer-Santos E, Durkin CH, Rigano LA *et al.* The *Salmonella* effector SteD mediates MARCH8-dependent ubiquitination of MHC II molecules and inhibits T cell activation. *Cell Host Microbe* 2016;**20**:584–95.

Bhutta ZA, Threlfall J. Addressing the global disease burden of typhoid fever. *JAMA* 2009;**302**:898–9.

Broz P, Ohlson MB, Monack DM. Innate immune response to Salmonella typhimurium, a model enteric pathogen. *Gut Microbes* 2012;**3**:62–70.

Burster T, Macmillan H, Hou T *et al.* Masking of a cathepsin G cleavage site in vivo contributes to the proteolytic resistance of major histocompatibility complex class II molecules. *Immunology* 2010;**130**:436–46.

Chakraborty S, Chaudhuri D, Balakrishnan A *et al.* *Salmonella* methylglyoxal detoxification by STM3117-encoded lactoylglutathione lyase affects virulence in coordination with *Salmonella* pathogenicity island 2 and phagosomal acidification. *Microbiology* 2014;**160**:1999–2017.

Chapman HA. Endosomal proteases in antigen presentation. *Curr Opin Immunol* 2006;**18**:78–84.

Cheminay C, Mohlenbrink A, Hensel M. Intracellular *Salmonella* inhibit antigen presentation by dendritic cells. *J Immunol* 2005;**174**:2892–9.

Cho KJ, Walseng E, Ishido S *et al.* Ubiquitination by March-I prevents MHC class II recycling and promotes MHC class II turnover in antigen-presenting cells. *P Natl Acad Sci USA* 2015;**112**:10449–54.

Coburn B, Grassl GA, Finlay BB. Salmonella, the host and disease: a brief review. *Immunol Cell Biol* 2007;**85**:112–8.

De Gassart A, Camosseto V, Thibodeau J *et al.* MHC class II stabilization at the surface of human dendritic cells is the result of maturation-dependent MARCH I down-regulation. *P Natl Acad Sci USA* 2008;**105**:3491–6.

de Waal Malefyt R, Haanen J, Spits H *et al.* Interleukin 10 (IL-10) and viral IL-10 strongly reduce antigen-specific human T cell proliferation by diminishing the antigen-presenting capacity of monocytes via downregulation of class II major histocompatibility complex expression. *J Exp Med* 1991;**174**:915–24.

Fujita H, Iwabu Y, Tokunaga K *et al.* Membrane-associated RING-CH (MARCH) 8 mediates the ubiquitination and

lysosomal degradation of the transferrin receptor. *J Cell Sci* 2013;**126**:2798–809.

Furuta K, Walseng E, Roche PA. Internalizing MHC class II-peptide complexes are ubiquitinated in early endosomes and targeted for lysosomal degradation. *P Natl Acad Sci USA* 2013;**110**:20188–93.

Gallois A, Klein JR, Allen LA *et al.* *Salmonella* pathogenicity island 2-encoded type III secretion system mediates exclusion of NADPH oxidase assembly from the phagosomal membrane. *J Immunol* 2001;**166**:5741–8.

Halici S, Zenk SF, Jantsch J *et al.* Functional analysis of the *Salmonella* pathogenicity island 2-mediated inhibition of antigen presentation in dendritic cells. *Infect Immun* 2008;**76**:4924–33.

Hernandez LD, Hueffer K, Wenk MR *et al.* Salmonella modulates vesicular traffic by altering phosphoinositide metabolism. *Science* 2004;**304**:1805–7.

Hess J, Ladel C, Miko D *et al.* Salmonella typhimurium aroA- infection in gene-targeted immunodeficient mice: major role of CD4+ TCR-alpha beta cells and IFN-gamma in bacterial clearance independent of intracellular location. *J Immunol* 1996;**156**:3321–6.

Hornick RB. Pathogenesis of typhoid fever. *J Egypt Public Health Assoc* 1970;**45**:247–59.

Inaba K, Inaba M, Romani N *et al.* Generation of large numbers of dendritic cells from mouse bone marrow cultures supplemented with granulocyte/macrophage colony-stimulating factor. *J Exp Med* 1992;**176**:1693–702.

Jabbour M, Campbell EM, Fares H *et al.* Discrete domains of MARCH1 mediate its localization, functional interactions, and posttranscriptional control of expression. *J Immunol* 2009;**183**:6500–12.

Lapaque N, Hutchinson JL, Jones DC *et al.* Salmonella regulates polyubiquitination and surface expression of MHC class II antigens. *P Natl Acad Sci USA* 2009;**106**:14052–7.

Ma JK, Platt MY, Eastham-Anderson J *et al.* MHC class II distribution in dendritic cells and B cells is determined by ubiquitin chain length. *P Natl Acad Sci USA* 2012;**109**:8820–7.

McCormick PJ, Martina JA, Bonifacino JS. Involvement of clathrin and AP-2 in the trafficking of MHC class II molecules to antigen-processing compartments. *P Natl Acad Sci USA* 2005;**102**:7910–5.

Majowicz SE, Musto J, Scallan E *et al.* The global burden of nontyphoidal *Salmonella gastroenteritis*. *Clin Infect Dis* 2010;**50**:882–9.

Mitchell EK, Mastroeni P, Kelly AP *et al.* Inhibition of cell surface MHC class II expression by *Salmonella*. *Eur J Immunol* 2004;**34**:2559–67.

Ni K, O'Neill HC. The role of dendritic cells in T cell activation. *Immunol Cell Biol* 1997;**75**:223–30.

Oh J, Shin JS. Molecular mechanism and cellular function of MHCII ubiquitination. *Immunol Rev* 2015;**266**:134–44.

Oh J, Wu N, Baravalle G *et al.* MARCH1-mediated MHCII ubiquitination promotes dendritic cell selection of natural regulatory T cells. *J Exp Med* 2013;**210**:1069–77.

Ravindran R, McSorley SJ. Tracking the dynamics of T-cell activation in response to *Salmonella* infection. *Immunology* 2005;**114**:450–8.

Redpath S, Angulo A, Gascoigne NR *et al.* Murine cytomegalovirus infection down-regulates MHC class II expression on macrophages by induction of IL-10. *J Immunol* 1999;**162**:6701–7.

Rescigno M, Urbano M, Valzasina B *et al.* Dendritic cells express tight junction proteins and penetrate gut epithelial monolayers to sample bacteria. *Nat Immunol* 2001;**2**:361–7.

Roche PA, Furuta K. The ins and outs of MHC class II-mediated antigen processing and presentation. *Nat Rev Immunol* 2015;**15**:203–16.

Rybicka JM, Balce DR, Chaudhuri S *et al.* Phagosomal proteolysis in dendritic cells is modulated by NADPH oxidase in a pH-independent manner. *EMBO J* 2012;**31**:932–44.

Savina A, Jancic C, Hugues S *et al.* NOX2 controls phagosomal pH to regulate antigen processing during crosspresentation by dendritic cells. *Cell* 2006;**126**:205–18.

Shin JS, Ebersold M, Pypaert M *et al.* Surface expression of MHC class II in dendritic cells is controlled by regulated ubiquitination. *Nature* 2006;**444**:115–8.

ten Broeke T, Wubbolts R, Stoorvogel W. MHC class II antigen presentation by dendritic cells regulated through endosomal sorting. *Cold Spring Harb Persp Biol* 2013;**5**:a016873.

Thibodeau J, Bourgeois-Daigneault MC, Huppe G *et al.* Interleukin-10-induced MARCH1 mediates intracellular sequestration of MHC class II in monocytes. *Eur J Immunol* 2008;**38**:1225–30.

Tobar JA, Gonzalez PA, Kalergis AM. Salmonella escape from antigen presentation can be overcome by targeting bacteria to Fc gamma receptors on dendritic cells. *J Immunol* 2004;**173**:4058–65.

Turk V, Stoka V, Vasiljeva O *et al.* Cysteine cathepsins: from structure, function and regulation to new frontiers. *Biochim Biophys Acta* 2012;**1824**:68–88.

Tze LE, Horikawa K, Domaschenz H *et al.* CD83 increases MHC II and CD86 on dendritic cells by opposing IL-10-driven MARCH1-mediated ubiquitination and degradation. *J Exp Med* 2011;**208**:149–65.

van Niel G, Wubbolts R, Ten Broeke T *et al.* Dendritic cells regulate exposure of MHC class II at their plasma membrane by oligoubiquitination. *Immunity* 2006;**25**:885–94.

Van Parys A, Boyen F, Verbrugghe E *et al.* *Salmonella* Typhimurium induces SPI-1 and SPI-2 regulated and strain dependent downregulation of MHC II expression on porcine alveolar macrophages. *Vet Res* 2012;**43**:52.

Vazquez-Torres A, Xu Y, Jones-Carson J *et al.* *Salmonella* pathogenicity island 2-dependent evasion of the phagocyte NADPH oxidase. *Science* 2000;**287**:1655–8.

Walseng E, Furuta K, Goldszmid RS *et al.* Dendritic cell activation prevents MHC class II ubiquitination and promotes MHC class II survival regardless of the activation stimulus. *J Biol Chem* 2010;**285**:41749–54.

Walseng E, Furuta K, Bosch B *et al.* Ubiquitination regulates MHC class II-peptide complex retention and degradation in dendritic cells. *P Natl Acad Sci USA* 2010;**107**:20465–70.

Walseng, E, Bakke, O, Roche PA. Major histocompatibility complex class II-peptide complexes internalize using a clathrin- and dynamin-independent endocytosis pathway. *J Biol Chem* 2008;**283**:14717–27.

Waterman SR, Holden DW. Functions and effectors of the *Salmonella* pathogenicity island 2 type III secretion system. *Cell Microbiol* 2003;**5**:501–11.

Zinngrebe J, Montinaro A, Peltzer N *et al.* Ubiquitin in the immune system. *EMBO Rep* 2014;**15**:28–45.